http://dx.doi.org/10.21577/0103-5053.20180229

J. Braz. Chem. Soc., Vol. 30, No. 3, 597-613, 2019
Printed in Brazil - ©2019 Sociedade Brasileira de Química

Article

Mixed Ternary Mononuclear Copper(II) Complexes Based on Valproic Acid with 1,10-Phenanthroline and 2,2'-Bipyridine Ligands: DNA Interaction and Cytotoxicity in V79 Cells

Claus T. Pich,[a,b] Paulo R. dos Santos,[c] Tatiana V. O. Fortunato,[b,d] Marilda Chiarello,[c] Iuri M. de Oliveira,[b,d] Bárbara Q. Soares,[a] Nour E. Ghermani,[e] Miriana Machado,[b,d] Mariana Roesch-Ely,[d] Françoise Dumas,[e,f] Hernan Terenzi,[g] João A. P. Henriques[b,c,d] and Sidnei Moura[*,c]

[a]Departamento de Energia e Sustentabilidade, Centro de Araranguá, Universidade Federal de Santa Catarina, Rod. Gov. Jorge Lacerda, 3201, Jardim das Avenidas, 88906-072 Araranguá-SC, Brazil

[b]Departamento de Biofísica e Departamento de Biologia Molecular e Biotecnologia, Universidade Federal do Rio Grande do Sul (UFRGS), 91501-970 Porto Alegre-RS, Brazil

[c]Laboratório de Produtos Naturais e Sintéticos, Instituto de Biotecnologia, Universidade de Caxias do Sul, 95070-560 Caxias do Sul-RS, Brazil

[d]Laboratório de Genômica, Proteômica e Reparo de DNA, Instituto de Biotecnologia, Universidade de Caxias do Sul, 95070-560 Caxias do Sul-RS, Brazil

[e]Laboratoire de Physique Pharmaceutique, Institut Galien Paris Sud, Université Paris Sud, CNRS, Faculté de Pharmacie, Université Paris Saclay, IPSIT, 92290 Châtenay-Malabry, Paris, France

[f]Laboratoire BioCIS, Faculté de Pharmacie, Université Paris Sud, CNRS, Université Paris Saclay, IPSIT, 92290 Châtenay-Malabry, Paris, France

[g]Centro de Biologia Molecular Estrutural (CEBIME), Departamento de Bioquímica, Universidade Federal de Santa Catarina, Campus Trindade, 88040-900 Florianópolis-SC, Brazil

This paper reports the DNA interaction and cytotoxicity of binary and ternary copper(II) complexes of valproic acid with phenanthroline or bipyridine and the complementary characterization of $Cu(Valp)_2Bipy$ by crystallography. Circular dichroism, plasmid and oligonucleotide assays have shown that the complexes interact with DNA in different manners and are able to cleave plasmid DNA and oligonucleotides at concentrations from 10 to 1000 mol L^{-1}. The plasmid DNA cleavage is enhanced 650, 375 and 285 times by photo activation with UVB light for the complexes $Cu(Valp)_2Phen$, $Cu(Valp)_2Bipy$ and $Cu_2(Valp)_4$, respectively. Cytotoxicity assays demonstrated that V79 cells were more sensitive to Cu^{II} derivatives than sodium valproate as evaluated by 3-(4,5-dimethylthiazol-2yl)-2,5-diphenyl tetrazolium bromide (MTT) and clonogenic assays, where the cytotoxic profile of the compounds was: $Cu(Valp)_2Phen$ higher than $Cu(Valp)_2Bipy$, higher than $Cu_2(Valp)_4$. Therefore, we report two copper complexes, which interact with DNA and promote its cleavage, leading to an enhanced cytotoxicity when compared to valproic acid.

Keywords: organometallic compounds, copper complexes, DNA interaction, plasmid cleavage

Introduction

The research on metals coordinated with organic molecules regularly used as drugs has increased in latest years.[1,2] In accordance with their features and affinity for biological goals, these coordination compounds may be more effective than the precursor organic molecules. The development of small molecules capable of catalyzing deoxyribonucleic acid (DNA) hydrolysis or oxidation at physiological conditions is important for the improvement of the therapeutically active agents.[3,4]

*e-mail: sidmoura@gmail.com

For this purpose, transition metal ions are some of the most important ions due to their role in various pathways as catalytic centers in enzymes and transition metal complexes, especially iron and copper. In addition, in their reduced oxidation state, transition metal ions can promote the formation of free radicals through Haber-Weiss or Fenton reactions.[5] The copper(II) is a Lewis acid and is one of the metals acting as an essential trace element involved in cellular respiration, antioxidant defense, neurotransmission, connective tissue biosynthesis and cellular iron metabolism.[6,7] Copper-based complexes have been investigated on the assumption that endogenous metals may be less toxic for normal cells than for cancer cells. The redox activity and affinity for binding sites that should be occupied by other metals makes copper to be toxic in some situations.[8]

It is generally believed that molecules which damage DNA or indirectly block DNA synthesis through inhibition of genes involved in processes that are important to DNA replication or repair, would make them better candidates for development as anticancer agents.[9-12] Several investigations provide evidence that Cu^{II} ions are capable of interacting directly with nuclear proteins and DNA, causing site-specific damage. It has been reported that copper compounds delay cell-cycle progression and increase cell death in different cell cultures, making copper complexes suitable for the development of antitumor drugs.[6-8,13] Moreover, other copper properties, as its glutathione decreasing activity, have been into focus on the drug resistance evasion, for example on glutathione (GSH)-dependent cisplatin resistance.[14,15]

Diimines, like 2,2'-bipyridine (Bipy) and 1,10-phenanthroline (Phen), have been used as ligands in several metal complexes due to their ability to interact with DNA as groove binders or even as intercalators and frequently inducing DNA cleavage.[16-18] Some complexes containing these ligands were described as being photoactive and that characteristic improves their DNA cleavage ability. Furthermore, photo-cleavage of nucleic acids by transition-metal complexes emerges as a field of great interest to improve the development of new therapeutic approaches.[19,20]

The valproic acid (VPA) is one of the oldest drugs used in seizure, bipolar disorder and migraine headaches therapy.[21] More recently, VPA has been described as an histone deacetylase (HDAC) inhibitor, that is able to alter expression of many genes.[22] The corresponding proteins could influence several important pathways such as cell cycle control, differentiation, DNA repair and apoptosis.[9] Furthermore VPA can silence DNA repair pathways, inactivate DNA repair proteins and induce reactive oxygen species (ROS) and DNA double strand breaks.[10] These characteristics lead to the investigation of VPA as a putative or adjuvant anticancer drug. In this way, some promising results were obtained, and several clinical trials are currently in progress using VPA in the treatment of different cancer types including leukemia and glioma.[9,23]

The first example of VPA complexation with metals was reported using Cu^{II} and bipyridine.[24] Cu^{II} also produces stable complexes with valproate ions (Cu-VPA) and some of them with aromatic imines afforded molecules with biological activity against microorganisms.[25] The high affinity of VPA for transition metals results in stable coordination compounds. The characteristic of carboxylate bond with metal cation (Lewis acid) is the short length between oxygen atoms and metallic core around 2.6 Å, responsible for the cluster chemical stability.[26]

The search for new active compounds Cu^{II}-based complex can be highlighted by recent studies. The ternary Cu^{II} complex was able to increase by more than three thousand times the anticonvulsant activity of VPA in mouse models of epilepsy.[27] Moreover, it exhibits discrete anti-inflammatory activity *in vivo*.[28] In other line, $Cu(Valp)_2Phen$ (compound **2**) and $Cu(Valp)_2Bipy$ (compound **3**) showed a good superoxide dismutase (SOD-like) mimetic *in vitro*.[29] Grünspan *et al.*[30] have demonstrated the teratogenic and mutagenic effects induced by similar complex of Cu^{II} on zebrafish (*Danio rerio*), which have shown the activity of these complexes on DNA and the interference caused in cell division.

Once, the complexes synthesized and studied in this work join ligands with different abilities to influence the DNA metabolism and stability. Searching for new active and secure drugs, this study aims the characterization of DNA interaction ability of the three VPA related complexes, their nuclease activity and the cytotoxicity in mammalian cells *in vitro* as preliminary studies for the development of a new series of molecules. The complementary chemical characterization of $Cu(Valp)_2Bipy$ complex (**3**) was also performed in order to complete the chemical data referring to these substances.

Experimental

Material and methods

VPA sodium salt (98%) was purchased from AK Scientific. All other chemicals used in this work, such as the aromatic imines Phen (99.5%) and Bipy (99.5%), Cu^{II} chloride dihydrate, 3-(4,5-dimethylthiazol-2yl)-2,5-diphenyl tetrazolium bromide (MTT) and the

solvents were purchased from Sigma-Aldrich®. Reagent-grade chemicals were used without further purification. Calf thymus DNA sodium salt (CT DNA) was used as obtained from Sigma Co. The plasmid pBSK II (2961 bp), used for DNA cleavage assays, was purchased from Stratagene, transformed into DH5 alpha *Escherichia coli* competent cells and amplified as previously described.[31] The plasmid DNA was extracted from *E. coli* and purified using Qiagen® Plasmid Maxi Kit protocol.[32] Infrared analysis were performed with a PerkinElmer® Spectrum 400 FTIR spectrometer using KBr pellet method. UV-Vis analyses were performed with a Beckman® DU 530 spectrophotometer (single beam) with quartz cuvettes (10 mm) using solutions at 10.0 μmol L^{-1} in chloroform.

Preparation of Cu^{II} compounds

$Cu_2(Valp)_4$ (complex **1**) was prepared according to Hadjikostas method (Scheme 1).[24] A solution of $CuCl_2.2H_2O$ (5.07 g, 29 mmol) in water (50 mL) was added over NaValp water solution (9.64 g, 58 mmol) with continuous stirring to form precipitate immediately. After 24 h, the powder was washed with pure water, and carried-out after vacuum filtration, then dried in a high vacuum chamber (0.02 mbar) for 24 h. Yield 99%; mp (differential scanning calorimetry, DSC) 290.3 °C; IR ν / cm^{-1} 2960(s), 2951(m), 2863(m), 1584(s), 1422(s); UV-Vis (chloroform) λ / nm 240-290.

The complexes **2** and **3** were prepared according to Veitía's method.[27] Two solutions of precursor salt (**1**) (4.0 g, 5.71 mmol) in dimethylformamide (DMF, 20 mL), were separately added with continuous stirring to Phen (2.26 g, 11.44 mmol) or Bipy (1.78 g, 11.43 mmol), previously solubilized in DMF (10 mL) at 80 °C. The Turkish-blue solutions were stored at room temperature. The light Turkish-green crystals of complex **2** was formed after 48 h and obtained by filtration and freeze-drying. Yield 88%; mp (DSC) 255-290 °C; IR ν / cm^{-1} 3057(w), 2959(s), 2934(m), 2870(m), 1569(s), 1514 (s), 1466(s); UV-Vis (chloroform) λ / nm 265. For complex **3**, the solvent was removed under vacuum. The dark Turkish-blue solid was dissolved in DMF (10 mL) with a few drops of methanol at 80 °C and stored at room temperature. Dark Turkish-blue crystals formed after 48 h were filtered and freeze-dried. Yield 99%; mp (DSC) 154.7 °C (Figure 1); IR ν / cm^{-1} 3447(m), 3112(w), 2956(s), 2929(m), 2871(m), 1610(s), 1570 (s), 1466(s); UV-Vis (chloroform) λ / nm 248, 298.

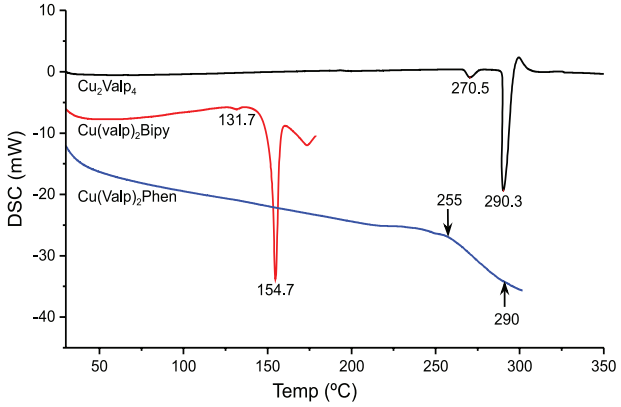

Figure 1. Differential scanning calorimetry (DSC) graphs for all compounds.

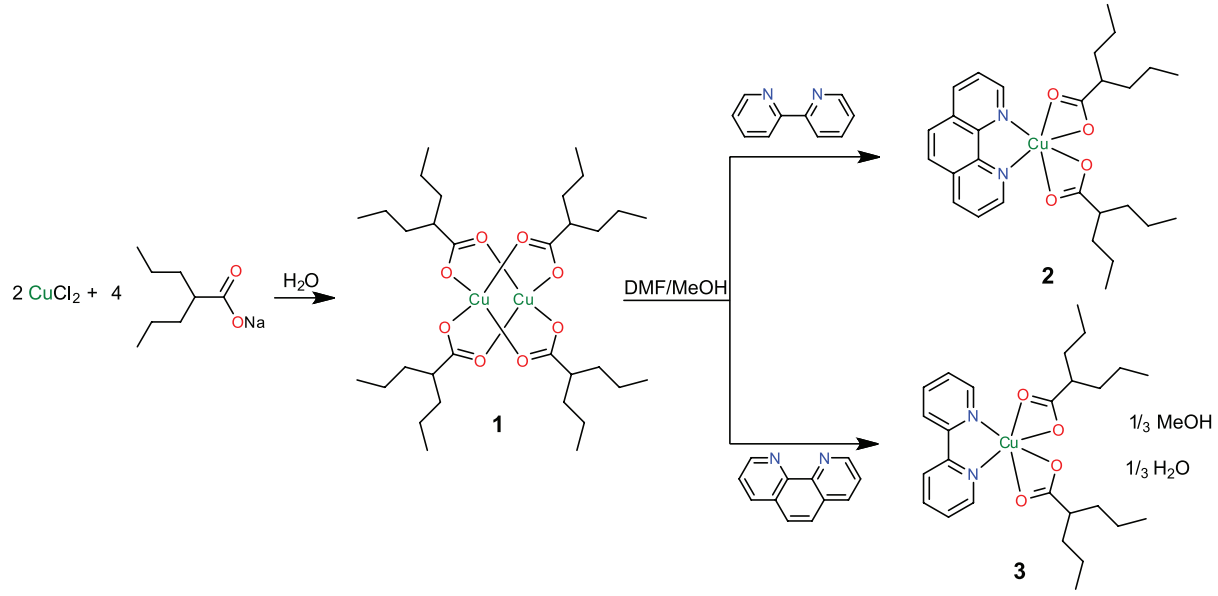

Scheme 1. Synthesis of Cu^{II} complexes.

Crystallography

Crystallographic analysis was performed in a diffractometer by single crystal technique. X-ray data were collected at 120 K (N_2 gas-stream) on a Bruker D8 Venture diffractometer using MoKα radiation (λ = 0.71069 Å). The Lorentz-polarization correction and the integration of the diffracted intensities were performed using APEX2 software suite,[33] which also includes SADABS[34] computer program for an empirical absorption correction. SORTAV[35] program was used for sorting and averaging data.[36] Details of the X-ray diffraction experiment conditions are given in Supplementary Information (SI) section. The crystal structure of the complex was solved using SIR94[37] program and refined using SHELX97[38] implemented in WinGX package.[39]

DSC analysis

Differential scanning calorimetry (DSC) analyses were performed in a DSC-60 Shimadzu device. Data were obtained using 5.0 mg in a N_2 atmosphere at 50 mL min^{-1}, 10 °C min^{-1}, range temperature 25-350 °C. Data were recorded in a rate time 1 s. Data were analyzed in OriginPro 2016 (test version).[40]

Chemical stability assay

In order to verify the chemical stability of the complexes in solution, molar conductivity parameter was used as the variable. The variation of conductivity over time indicates molecular breaks by ionization/dissociation or polymerization. The molar conductivities of the Cu^{II} complexes were measured in solution over a period of 120 h.[41] Solutions of the compounds **1**, **2** and **3** were prepared in ethanol 99% and dimethylsulfoxide (DMSO) at a concentration of 4.0 mmol L^{-1}. These solvents were used in order to achieve the concentration needed for the testing once the solubility of the complexes in pure water is very restricted. The solutions were stocked in closed glass vials (Schott Duran® 25 mL) without headspace and maintained at 37 °C full time of the experiment. Specific conductivities (κ) were measured periodically on a Hydraulis® MCA-150 conductivity meter. The molar conductivities (Λ) were calculated according to the equation 1, where κ is the specific conductivity of the solution and c is the concentration of the complex:[42]

$$\Lambda\ (S\ cm^2 mol^{-1}) = \frac{\kappa\ (S\ cm^{-1})}{c\ (mol\ cm^{-3})} \quad (1)$$

DNA interaction activity: plasmid cleavage activity assays

Plasmid DNA pBSK II (Stratagene) was obtained and purified according to standard techniques.[43] The DNA cleavage ability of the complexes **1**, **2**, **3** and the reference NaValp, all diluted in 20% acetonitrile (ACN), were examined in order to establish the influence of pH and concentration in the conversion of pBSK II supercoiled DNA (F I) to the open circular (F II) and linear DNA (F III) using agarose gel electrophoresis to separate the cleavage products.[44] Exploring experiments were designed in accordance to the proceedings calculated using the Design-Expert 7.0 program.[45] In general, 300 ng of pBSK II DNA (30 μmol L^{-1} bp) in 10 mmol L^{-1} Hepes Buffer pH 7.0, 7.5 and 8.0 were treated with complexes at 10, 255 and 500 μmol L^{-1} concentrations, in a final concentration of 10% ACN at 37 ºC, in absence of light (AL) for 12 h and UVB light (UV) for 5 min using a BIORAD® transiluminator UV 302 T26M apparatus with a UVB peak ranging from 300 to 312 nm at 50% light power. ACN was used in order to dissolve the complexes on the concentration needed once the solubility of them in pure water is very restricted. All the assays were conducted using freshly prepared solutions and included two control reactions: one only with nano-pure water (Milli-Q®) and the other with 10% ACN, both without complex, to serve as a reference of spontaneous plasmid DNA fragmentation. Thereafter, each reaction was quenched by adding 4 μL of a loading buffer solution (50 mmol L^{-1} Tris-HCl pH 7.5, 0.01% bromophenol blue, 50% glycerol and 250 mmol L^{-1} ethylenediamine tetraacetic acid (EDTA)) and then subjected to electrophoresis on a 1.0% agarose gel containing 0.3 μg mL^{-1} of ethidium bromide in 0.5 × tris-borate-EDTA (TBE) buffer (44.5 mmol L^{-1} Tris pH 8.0, 44.5 mmol L^{-1} boric acid and 1 mmol L^{-1} EDTA) at 90 V for 1.5 h. The resulting gels were visualized and digitized using a DigiDoc-It gel documentation system (UVP) (KODAK). The proportion of plasmid DNA in each band was quantified using Kodak Molecular Imaging Software 5.0 (Carestream Health). The quantification of supercoiled DNA (F I) was corrected by a factor of 1.47, since the ability of ethidium bromide to intercalate into this DNA topoisomeric form is decreased relative to open circular and linear DNA.[2] The results were expressed as graphic representations of the best correlation of the two parameters, concentration and pH, in order to maximize the Form III (linear) plasmid DNA. Experiments were performed with NaValp in order to evaluate the activity of the ligand itself. The ligands Bipy and Phen were already analyzed and no activity was observed.[19] The best performance point (maximization of F II and F III of the plasmid DNA) was calculated using the Design Expert 7.0® program[45] and the

results were used to select the best conditions to perform the following tests. The effect of concentration was then tested at 0, 25, 50 and 100 μmol L^{-1}. All the following experiments of plasmid DNA cleavage were performed at pH 7.5 and 37 °C.

The kinetics of plasmid DNA cleavage performed by complexes **1**, **2** and **3** were evaluated following the loss of supercoiled DNA fraction along the reaction time under a single concentration of complex along the time. AL samples were collected within 60 min intervals and UV samples at 20 s intervals. The apparent plasmid DNA cleavage rates (kobs) were obtained from the plot of LN-[supercoiled DNA (%)] *versus* time. The concentration used was 50 μmol L^{-1} and the other reaction conditions were identical to those described above. The incubations were submitted to agarose gel electrophoresis and analyzed.[2] Results were also expressed as K_2.

To investigate the need of O_2 to cleave DNA, samples were incubated in anaerobic conditions. For anaerobic DNA cleavage assays, a two-step procedure was used to obtain deoxygenated conditions. All solutions and reaction mixtures containing 50 μmol L^{-1} of complex **1**, **2** or **3** were prepared in an argon filled glove bag. Samples in AL were then incubated in a sealed argon-filled vacuum desiccator for 1 h and in UV were sealed with Parafilm® and exposed immediately for 1 min. Fe(EDTA) was used as a positive control for DNA damage via radical processes. A negative control, that is incubation without complex, was always performed. As a control reaction the same procedures were executed in O_2 atmosphere. All other conditions and procedures were essentially the same as those described for former reactions.[46]

In order to evaluate the formation of hydroxyl radical species by the complexes, experiments were conducted in AL and UV with and without 10% of DMSO in the reaction.[19] The samples were incubated in AL for 1 h and in UV for 1 min then submitted to gel electrophoresis and analyzed as described above.

In order to investigate the contribution of electrostatic interactions in the plasmid DNA cleavage promoted by complexes **1**, **2** and **3**, assays were conducted as described above but with an increase in the ionic strength of the reaction media by the addition of NaCl and $LiClO_4$ (from 25 to 200 mmol L^{-1}). Incubations were performed in triplicate in AL for 12 h and UV for 60 s.

Oligonucleotide cleavage assay

Aiming to obtain additional data about the way of DNA cleavage and preferential sites to act, plasmid DNA was substituted by a synthetic oligonucleotide of 49-mer (bp) that perform a region of double helix of 21 bp, equivalent to two complete turns of DNA helix, one A-T and the other C-G and a poly T loop at one extremity. At the 5' extremity, a fluorescent marker (FAM) is covalently attached. The cleavage reaction was performed at pH 8.0, 37 ºC for 1 h, at concentrations of 0, 5, 50 and 500 μmol L^{-1}, under AL since the fluorescent marker is highly sensitive to UV light.[20] Negative controls were reactions containing only the solvent, incubated or not.

Circular dichroism DNA interaction assay

Circular dichroism (CD) is a method able to detect alterations in optical activity of chiral molecules using its interaction with circularly polarized electromagnetic rays. The B-form conformation of CT-DNA shows two CD bands in the UV region, a positive band at λ 278 nm due to base stacking and a negative band at λ 246 nm due to polynucleotide helicity.[47]

The experiments were performed as described in the literature with small alterations.[20] One sample of 200 μmol L^{-1} CT-DNA in 10 mmol L^{-1} of HEPES buffer were titrated with the Cu^{II} complexes (**1**, **2** and **3**) in concentrations ranging from 19.80 to 181.82 μmol L^{-1} (molar ratios of 0.1 to 1.0) and 0 (negative control). The start material NaValp was tested in molar ratios of 0.50 to 5.00. The screenings were performed ranging from λ 220 to 600 nm at 37 °C immediately after the addition of the complexes. Results were plotted on tables and graphics presenting the regions of major interest were produced. Spectra containing only the complexes and DNA with growing concentrations of solvent (ACN) were performed as control reactions.

Spectrophotometric UV-Vis DNA interaction assay

Absorption titration measurements were done by varying the concentration of CT DNA but keeping the metal complexes in 10% ACN and 10 mmol L^{-1} HEPES buffer pH 7.5 concentration as constant (50 μmol L^{-1}) and using the concentrations of 0, 12.5, 25.0, 37.5, 50.0, 66.5, 75.0, 87.5 and 100 μmol L^{-1} of CT-DNA. The base line was performed with the mixed solvent and parallel measurements with the solvent and CT-DNA to eliminate the absorbance of DNA itself (Figure S11, SI section). The solutions were allowed to incubate for 60 min before the absorption spectra were recorded. The experiments were repeated three times and the results obtained were plotted in tables and shown on graphics.

Cytotoxicity assays: V79 cell culture and treatments

V79 cells were cultured under standard conditions in Dulbecco's modification of Eagle medium (DMEM) supplemented with 10% heat-inactivated fetal bovine serum

(FBS), 0.2 mg mL^{-1} L-glutamine, 100 IU mL^{-1} penicillin and 100 μg mL^{-1} streptomycin. Cells were kept in tissue-culture flasks at 37 °C in a humidified atmosphere containing 5% CO_2 in air and were harvested by treatment with 0.15% trypsin-0.08% EDTA in phosphate buffered saline (PBS) buffer. The compounds were dissolved in DMSO or ethanol and added to the medium to reach the different desired concentrations. The final DMSO or ethanol concentration in the medium never exceeded 0.2%, and the control group was exposed to an equivalent concentration of solvent. Cells were incubated at 37 °C for 72 h with NaValp (500, 1000, 1500 and 2000 μmol L^{-1}), **1** (50, 100, 150 and 200 μmol L^{-1}), **2** (1, 1.5, 2, 5, 7.5 and 10 μmol L^{-1} to MTT assay or 1.5, 2.5, 3.5, 4.5 and 5.5 μmol L^{-1} to clonogenic assay) or **3** (50, 100, 150 and 200 μmol L^{-1}). The corresponding vehicles, distilled H_2O, 0.5% DMSO and 0.5% ethanol were used as negative controls to NaValp, **1**, **2** and **3**, respectively.

Cytotoxicity evaluation in V79 cells using MTT assay

Chinese Hamster lung fibroblast cells (V79) were seeded at 5×10^3 cells *per* well in DMEM at 10% FBS in 24-well plates. After 24 h, the medium was removed and cells were exposed to the compounds as previously described.[48] After the exposure, cells were washed once with PBS buffer before adding 0.1 mL serum-free medium containing 1 mg mL^{-1} yellow tetrazolium salt MTT dye to each sample. After incubation for 4 h, the supernatant was removed, and the obtained purple formazan product was dissolved in 1 mL ethanol, stirred for 15 min, and the absorbance was read at λ 540 nm. This assay measures the activity of cellular dehydrogenases (mainly from mitochondria) and, indirectly, the cell viability. The method is based on the reduction of MTT salt. It provides a quantitative measure of the number of metabolically viable cells. The results were expressed as the percentage of cell viability in relation to the respective negative control.

Clonogenic assay

We assessed the ability of cells to form colonies on a monolayer surface into a well of a 6-well plate. Cells were plated at a density of 200 cells *per* well and allowed to adhere. After 24 h, the medium was removed and cells were exposed to the compounds as previously described.[49] After the exposure period, cells were maintained in drug free medium for 5-7 days. After that, cells were fixed in methanol and stained with crystal violet. Colonies were manually counted, and survival were presented as a percentage relative to the respective negative control.

Statistical analysis: DNA interaction assays

Each experiment was carried out in triplicate. The analysis of the results obtained from the plasmid DNA cleavage assays at various pH values and concentrations were performed with the program Design-Expert 7.0 Statistical[45] analysis and the other plasmid experiments was conducted by ANOVA followed by Dunnett's multiple comparison test. The GraphPad Prism 6.0 software[50] was employed and p value under 0.05 was considered significant.

Statistical analysis: cytotoxicity assays

Each experiment was carried out in triplicate. Statistical analysis was conducted by ANOVA followed by Dunnett's multiple comparison tests. Results were considered significant when p value is under 0.05 (the smaller the p-value, the higher the significance). The GraphPad Prism 6.0 software[50] was employed.

Results and Discussion

Crystallographic studies

A new procedure for crystallization of the compound **3**, have produced a single crystal in solvate phase with methanol and water molecules in the crystal matrix. Molecular structure and crystallographic data of complex **2** were already disclosed.[27,29] Complex **3** crystallizes in the monoclinic space group P21/n (SI 1) with three independent mononuclear spatial forms of the complex in the asymmetric unit as shown in Figure 2. One water molecule and a part of methanol (without resolved H atoms) were also found in the asymmetric unit.

Table S1 (SI section) gives selected bond distances and angles around the copper atoms (see for atom labels). Two Valp and one Bipy ligands are attached to each of the three Cu^{II} atoms in nearly octahedral geometries. A similar coordination was recently reported for Zn-Valp-N-donor ligands complexes.[51] The Cu–O and Cu–N bond distances and angles are equivalent for the three metal atoms. Six Valp moieties, grouped exactly in the middle of the unit cell, were the aliphatic chains that form the center of cell (Figure 3). Crystal data was deposited in the Cambridge Crystallographic Data Center (code CCDC 1507321).

Chemical stability assay

To ensure that the complexes are stable for long periods of incubation, mainly in the cytotoxicity experiments,

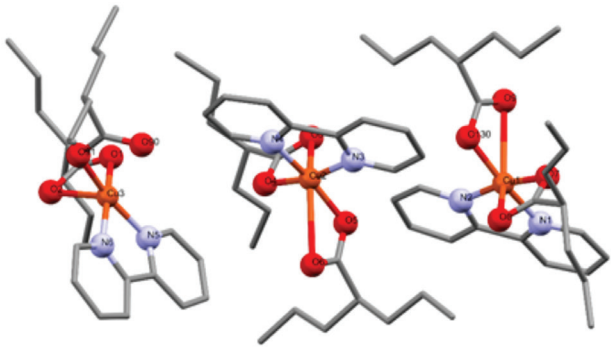

Figure 2. Asymmetric unit of complex **3** (water and methanol were omitted for clarity).

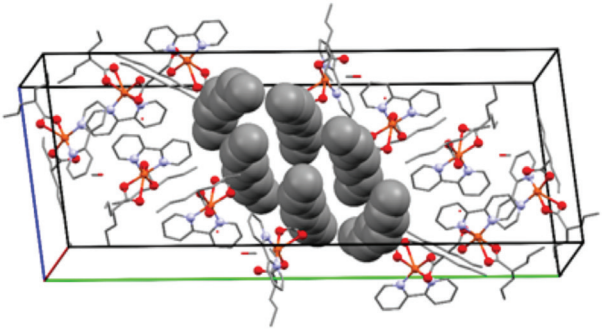

Figure 3. The crystal packing of the compound **3**. Cell vectors are indicated. The valproate carbons are displayed in the space fill mode. Hydrogen atoms are omitted for clarity.

molecular conductivity (Λ) experiments were performed. The results obtained are shown on Figure 4 and according to Dean[42] indicate that they are not electrolytes. Therefore, maintaining the apparent molar conductivity as a function of time without increasing or decreasing trend indicates that they are stable to dissociation or solution ionization over a period of 120 h.

Some intrinsic factors that may affect the mobility of electrical charges in the solution, such as the differences in pK_a of the solvents, presence of water or the conformation of the sphere of solvation of the complex molecules.[52] Such factors may explain the variations of mean values of molar conductivity of the same compound in different solvents.

DNA interaction activity: plasmid cleavage activity assays

As a first step the complexes **1**, **2** and **3** were tested in respect to their ability to cleave supercoiled plasmid DNA (F I), forming circular open (F II), linear (F III) or even breaking the DNA almost completely. For that purpose, the Design-Expert 7.0 program®[45] was used and the results expressed as surface graphics (Figures S3, S4 and S5, SI section). NaValp used as ligand control was tested only by classical methods in the absence of light (AL) (Figure S1, SI section) and UVB light (Figure S2, SI section). In the same experiment the solvent (0) used in the reactions was tested against water (nc) to certify that it does not modify the proportion of the DNA forms and no significative result was observed (Figures S1 and S2, SI section). It can be observed the effectiveness of the complexes **1**, **2** and **3**, respectively, in pH ranging from 7.0 to 8.0, concentrations ranging from 10 to 500 μmol L^{-1} and in AL and UV. All the complexes in all conditions presented DNA cleavage ability but they are partially inhibited in the concentration of 500 μmol L^{-1} or higher. The presence of UV enhances the activity of the three complexes, but **1** was the less sensitive. Usually Phen and Bipy complexes also show this photo induction behavior due to the ability of these molecules to absorb UV.[5,16,20,53] The best fit for concentrations and pH according to calculations using the Design-Expert 7.0 program®[45] are: (**1**) AL 326.63 μmol L^{-1} and pH 7.55, UV 349.18 μmol L^{-1} and pH 7.96; (**2**) AL 284.07 μmol L^{-1} and pH 7.45, UV 293.93 μmol L^{-1} and pH 7.74; (**3**) AL 300.77 μmol L^{-1} and pH 7.58, UV 309.38 μmol L^{-1}

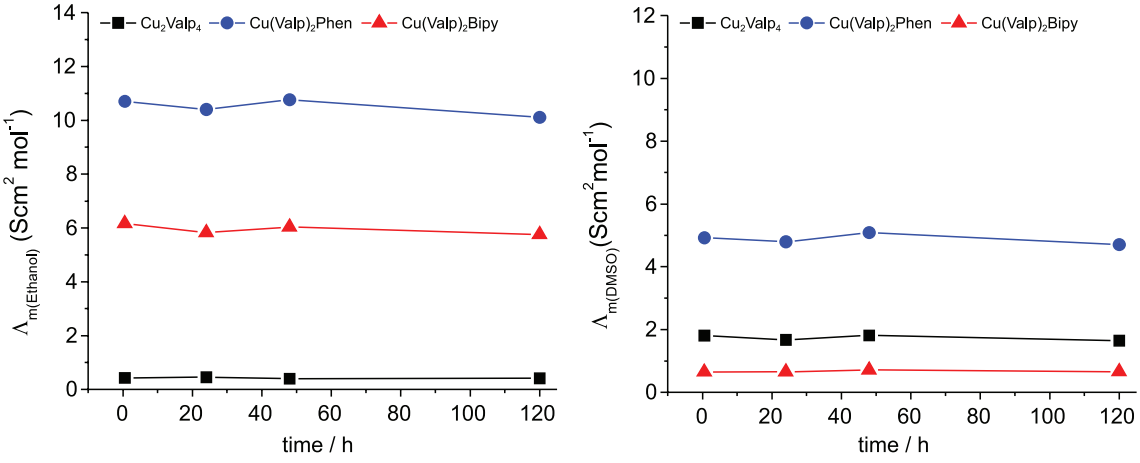

Figure 4. Molar conductivity variance of the three copper complexes in ethanol and DMSO during 120 h.

and pH 7.50. NaValp was also tested in concentrations ranging from 0 to 500 μmol L^{-1}, but no significant result was obtained (Figures S1 and S2, SI section). Considering the obtained results, experiments were accomplished in AL and UV at pH 7.5 using concentrations ranging from 25 to 100 μmol L^{-1} in order to obtain more accurate data from the activity of the complexes. The results in AL were obtained after 12 h of incubation and show the influence of both N-donor ligands to increase the ability to cleave the plasmid DNA molecule as reported in other publications from different groups.[2,54,55] Both complexes **2** and **3** (Figures 5b and 5c) presented even a slight inhibition of the activity at the higher concentration probably due to the precipitation of the complexes in the presence of DNA. Incubation in the presence of UV, as shown before, enhances the activity of the complexes, once the results obtained after only a minute incubation were almost the same as those obtained after 12 h incubation in AL. This clearly demonstrates an enhancing effect of UV-light when comparing the reaction time of DNA photo cleavage conditions (UV) *versus* the standard cleavage conditions (AL) probably related to the N-donor ligands. This result can also be influence of the metal photoactivation itself, since **1**, that is composed only of Cu^{II} and VPA, presented an increase on its activity. Certainly, all these factors contribute to it in complexes **2** and **3** because their increase in activity is higher than **1**.[19,54] The VPA control was not able to be photoactivated demonstrating that this ligand does not have influence on this matter (Figure S2, SI section).

Kinetic studies of **1**, **2** and **3** were performed at 50 μmol L^{-1} concentration. The graphic representations of the kinetic results in AL and UV are shown in Figure 6. The kinetic observed (K_{obs}) obtained for **1**, **2** and **3** were in AL: 7×10^{-6}, 2×10^{-5}, 4×10^{-5} s^{-1} and in UV 2×10^{-3}, 1.3×10^{-2}, 1.5×10^{-2} s^{-1}, respectively. In the experiments in AL a slight difference in activity of the complexes **1**, **2** and **3** can be noted and it is probably due to the presence of the N-donor ligands that increase the ability to cleave DNA (Figure 5). The photo activation promoted by UV increases the activity of the three complexes (Figure 7). The effect is more pronounced for **2** and **3** where an increase of the plasmid DNA cleavage is enhanced 650 and 375 times, respectively. For **1** the enhancement was 285 times, however, the activity was always 10 times lower. The results agree to the experiments shown before and differences in the photo activation effect of the complexes are probably due to the presence of aromatic ligands in **2** and **3**, as previously mentioned and the effect of the different N-donor ligands used.

Complexes **1**, **2** and **3** were incubated in the absence and in the presence of DMSO, a hydroxyl radical scavenger, and the results of **2** and **3** show reduction of activity when DMSO was present, which suggests the participation of hydroxyl radicals on the process even in AL or UV (Figure 8). Similar results can be observed in other 2,2-bipyridine and 1,10-phenantroline complexes with ROS involved in the cleavage. In these cases, the hydroxyl radical was not the only one present in the reaction.[19] It can be observed that the more pronounced effect occurred in the incubations of **3** under UV conditions and this also suggest that this complex is more dependent on the formation of ROS. These can be due to the ability of Phen complexes to intercalate, even in a weak form, in the double chain of DNA and therefore be more independent of the formation of ROS.[19,20,54]

Aiming to observe if the complexes need oxygen to generate the reactive species observed in DMSO

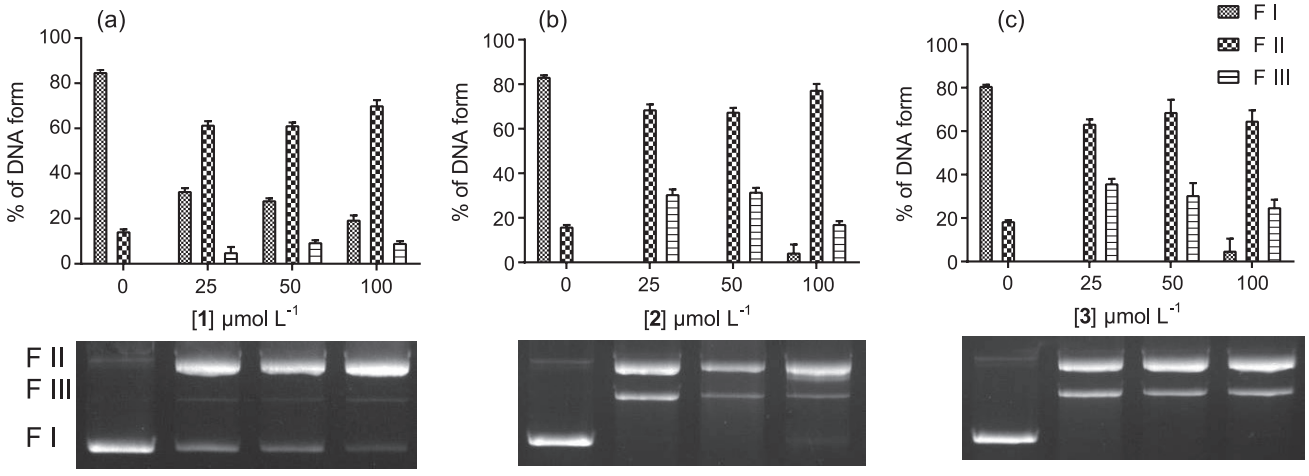

Figure 5. Plasmid DNA cleavage assay of complexes **1** (a), **2** (b) and **3** (c) incubatedin absence of light, pH 7.5, concentrations of 0 (negative control), 25, 50 and 100 μmol L^{-1} (left to right) for 12 h at 37 ºC. The graphical results are a medium obtained from three analyses. It can be observed that all complexes cleave DNA in the concentrations tested but complex **1** is the less active of the three. Complexes **2** and **3** suffered a light inhibition on the highest concentration (100 μmol L^{-1}).

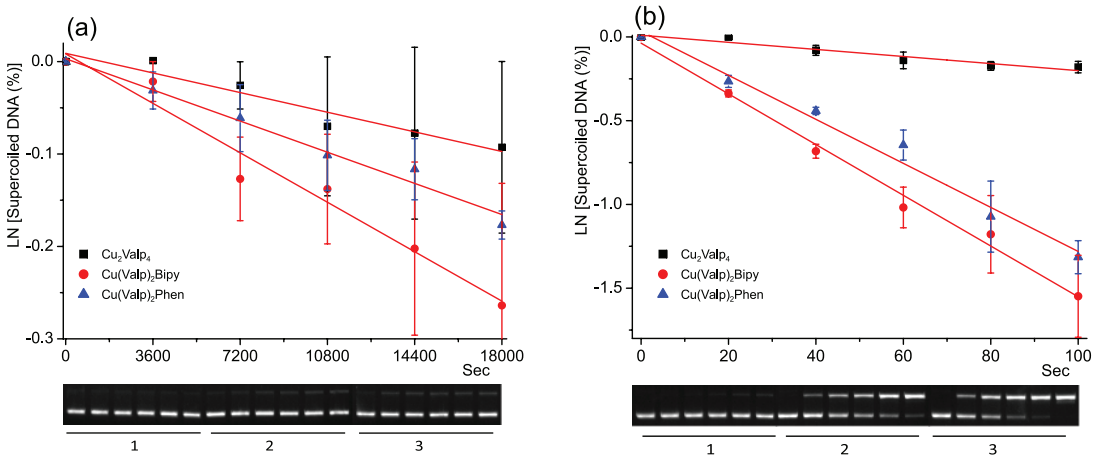

Figure 6. Kinetic studies plasmid DNA cleavage of complexes **1**, **2** and **3** were performed at 50 μmol L^{-1} concentration of complexes in (a) AL and (b) UV. The K_{obs} obtained for **1**, **2** and **3** were (a) AL 6×10^{-6}, 1×10^{-5}, 5×10^{-5} s^{-1}, respectively; (b) UV 2×10^{-3}, 1.3×10^{-2} and 1.5×10^{-2} s^{-1}, respectively. In the experiments in AL a slight difference in activity of the complexes **1**, **2** and **3** can be noted and it is probably due to the presence of the N-donor ligands that increase the ability to interact with DNA. The photoactivation promoted by UV increases the activity of the three complexes and it is more pronounced in **2** and **3** probably due to the presence of N-donor ligands.

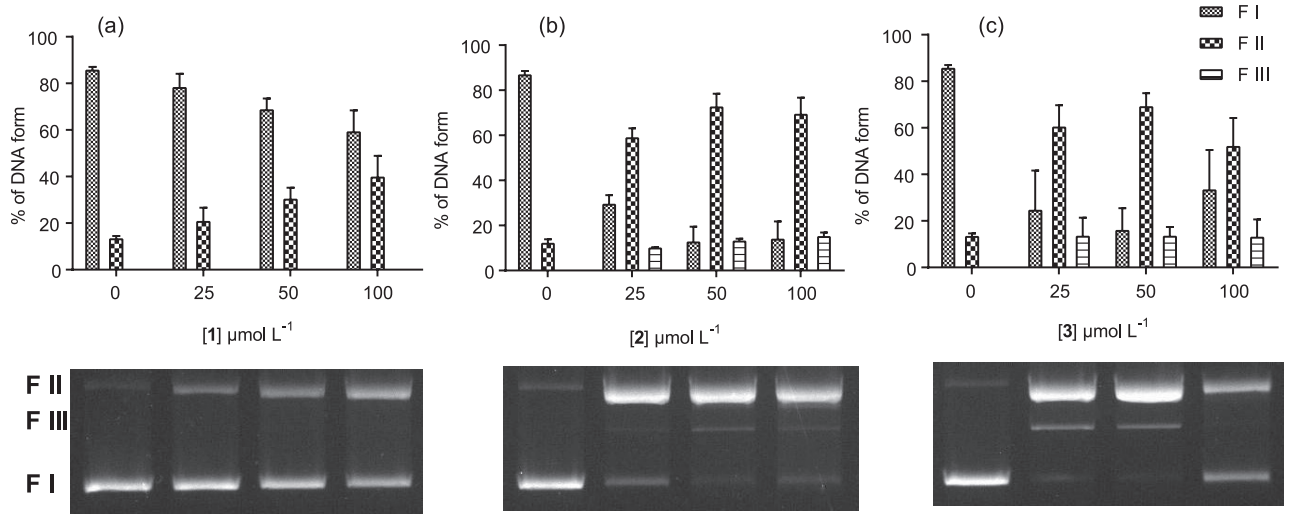

Figure 7. Plasmid DNA cleavage assay of complexes **1** (a), **2** (b) and **3** (c) incubated in presence of UV light, pH 7.5, concentrations of 0 (negative control), 25, 50 and 100 μmol L^{-1} (left to right) for 1 min at 37 ºC. The graphical results are an average obtained from three analyses. It can be observed that all complexes cleave DNA in the concentrations tested, but complex **1** is far the less active of the three. Complexes **2** and **3** suffered an inhibition on the highest concentration (100 μmol L^{-1}) that is bigger than the absence of light.

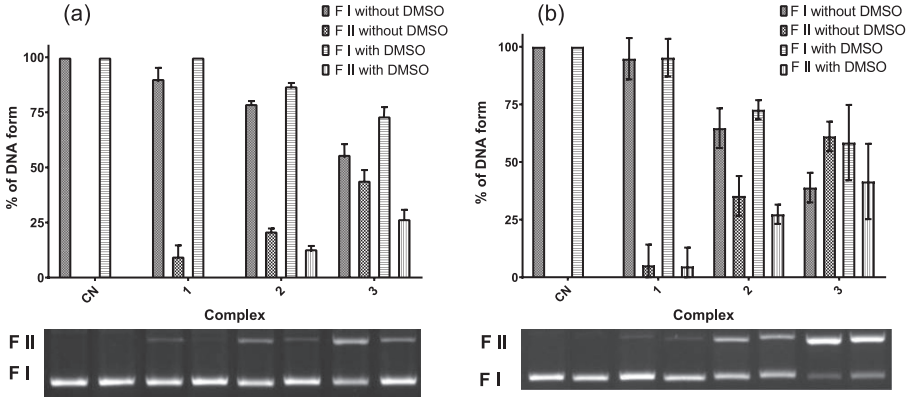

Figure 8. Plasmid DNA cleavage assay of complexes **1**, **2** and **3** incubated in absence and in presence of DMSO, a hydroxyl radical scavenger. Negative control (NC) with only ACN, **1**, **2** and **3** (50 μmol L^{-1}) were incubated with and without 10% DMSO for 12 h in AL (a) and 1 min in UV (b). Complexes **2** and **3** show reduction of activity when incubated in presence of DMSO suggesting the participation of hydroxyl radicals on the process even in AL or UV.

experiments anaerobic DNA cleavage assays were performed (Figure 9). Samples were incubated in argon atmosphere and oxygen atmosphere in AL and UV. The complexes presented ability to cleave DNA in the absence of oxygen in both conditions, indicating that the cleavage activity occurs under UV light or in dark conditions. Only **2** under UV suffered an inhibition in argon atmosphere but maintaining its activity (Figure 9c). Several evidences in this work indicate that the activity of the complexes is due to oxidation, but the presence of activity in argon atmosphere leads to the conclusion that different reaction mechanisms may occur and some of them should be oxygen independent. Similar results have been described where copper(II) metal complexes with heterocyclic N-donor ligands also presented activity in AL or UV and in the absence of oxygen.[56]

The influence of electrostatic properties in the ability of **1**, **2** and **3** was tested by addition of NaCl and $LiClO_4$ in a range of 25 to 200 mmol L^{-1} to the reaction medium. When NaCl or $LiClO_4$ is added, the proportion of supercoiled DNA increases and the cleaved DNA falls down, indicating a proportional decrease of the plasmid DNA cleavage promoted by the complexes following the gradual increase in ionic strength. The plasmid cleavage in the presence of NaCl and $LiClO_4$ was lower than the control reaction (nc) for **1** in AL conditions (Figures S6a and S6c, SI section), but this effect cannot be observed under UV (Figures S6b and S6d, SI section) probably due to the low increase of activity in this condition and the shorter incubation time. Complexes **2** and **3** show inhibition in both conditions (AL and UV) and in the presence of NaCl (Figures S7 and S8, a and b, SI section) and $LiClO_4$ (Figures S7 and S8, c and d, SI section). The stronger effect can be observed in **3** indicating that this complex is more dependent of electrostatic interactions.

Oligonucleotide cleavage assay

Cleavage assay was performed to access the complex ability to cleave oligonucleotide DNA. Incubations were

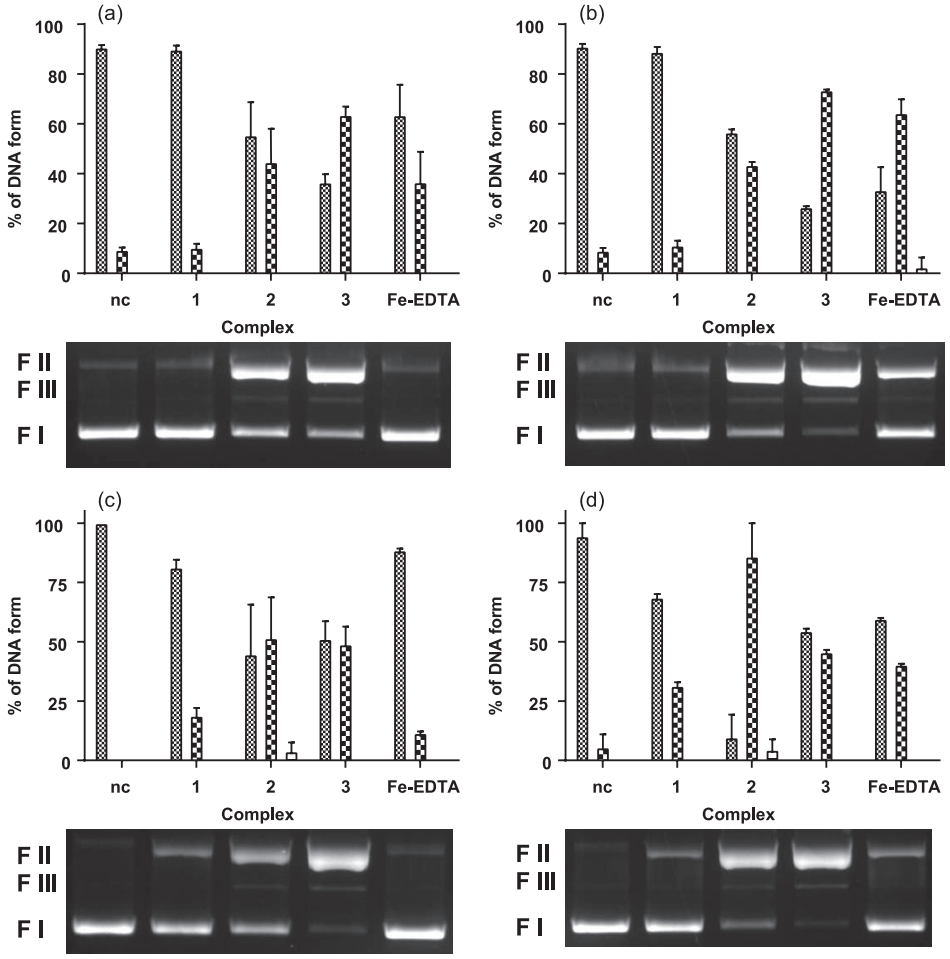

Figure 9. To investigate if the complexes need oxygen to cleave plasmid DNA assays were performed in argon atmosphere (a) and (c) and as a control in oxygen atmosphere (b) and (d) in AL (a) and (b) and UV (c) and (d). Incubations were performed in AL for 60 min and in UV for 1 min. Only **2** under UV suffered an inhibition in argon atmosphere, but maintaining its activity.

performed in absence of light as described above at three different concentrations for each complex (500, 50 and 5 μmol L^{-1}). All the complexes show an unspecific cleavage pattern of DNA directly correlated to the concentration of complexes (Figure 10). These findings may be correlated to oxidative cleavage of the DNA oligonucleotide, since the generation of ROS, in many cases, promotes unspecific fragmentation.[57]

Circular dichroism experiments

The effect of the complexes on the secondary structure of DNA was verified by circular dichroism (CD) spectroscopy. The three complexes showed alterations both in the λ 245 and 275 nm bands that are associated to the helicity and base-pair stacking, respectively.[58] The NaValp, used as ligand control, does not show any visible alteration on the DNA structure (Figure S9, SI section). ACN titration was performed as a control of the effect of the solvent over DNA and only a very slight reduction of the curves was detected due to the dilution of the solution (Figure S10, SI section). The complexes were also titrated alone (no DNA) as a control. No significant results were found (Figures S11, S12 and S13, SI section).

The results presented by the three complexes are quite different when compared to each other and to the control. Sodium valproate is not able to induce changes in both bands that are normally presented by CT-DNA (Figure S9, SI section). Complex **1** promotes a reduction of the intensity of both λ 245 and 275 nm bands. This primarily suggests groove binding nature of the complexes (Figure 11a).[19,59] Complex **2** induces a remarkable hyperchromic effect on the λ 275 nm band of DNA, associated with base-pair stacking, suggesting stabilization of this secondary structure (Figure 11b).[20] The band at λ 245 nm, relative to the right handed helicity of B-DNA was also partially affected, showing a red shift after addition of the complex. Intercalators normally present a movement in direction to the zero line on this band and the result obtained cannot be explained by intercalation events. This complex also induces the formation of a new peak near the λ 310 nm region probably an induced circular dichroism (ICD) event. These results suggest that **2** can act as an intercalator, but other ways of interaction with the DNA molecule are involved.[20] Complex **3** (Figure 11c) promotes a red shift of the positive and negative bands with a slight hypochromism on the second one indicating an electrostatic interactions corroborating with the results of the influence of electrostatic properties presented on SI 8.[60] It also gives origin to a new peak in between λ 305 and 320 nm that is also probably an ICD event that is related to the acquisition

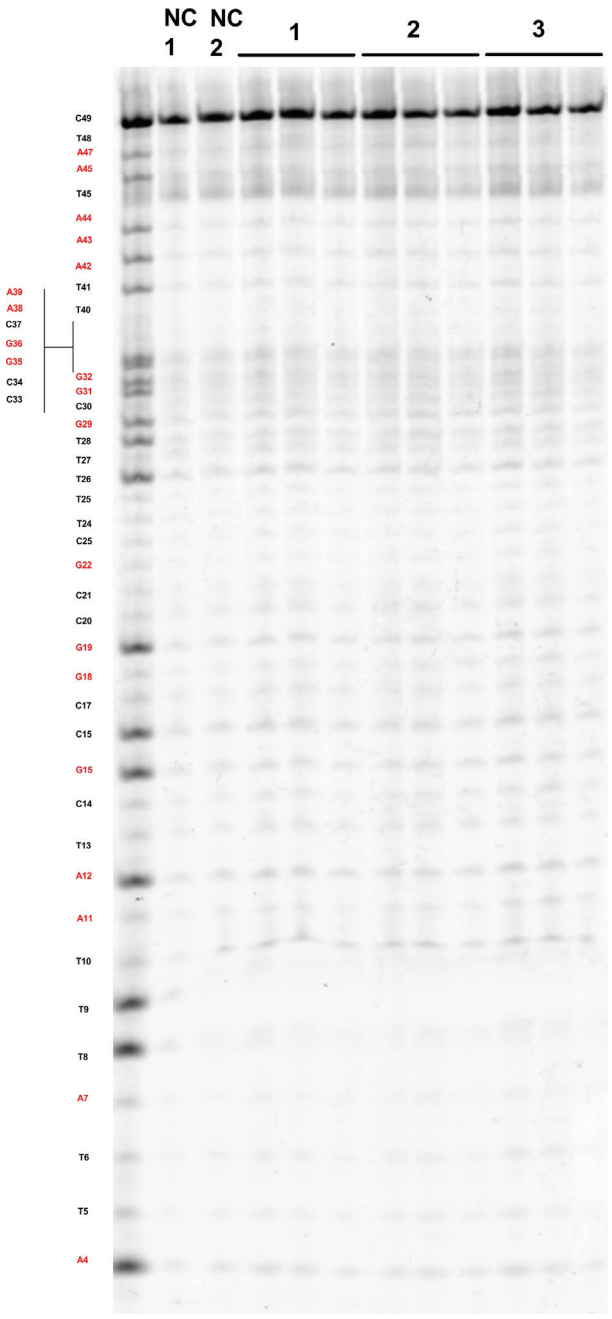

Figure 10. Oligonucleotide cleavage assay results. The cleavage of the oligonucleotide in all sites producing a small increase in all electrophoretic bands characterizes the activity as resultant from oxidative species that do not have a specific site to act. Two types of negative control were used: NC 1: absence of non-incubated complex; NC 2: complex incubated. Complexes **1**, **2** and **3** were tested in concentrations of 500, 50 and 5 μmol L^{-1}, respectively.

of CD signal by the complex and need more studies to be solved.[58,61]

UV-Vis spectrophotometric assay

The results obtained in UV-Vis spectrophotometric assays are shown on Figure 12. Both **2** and **3** presented

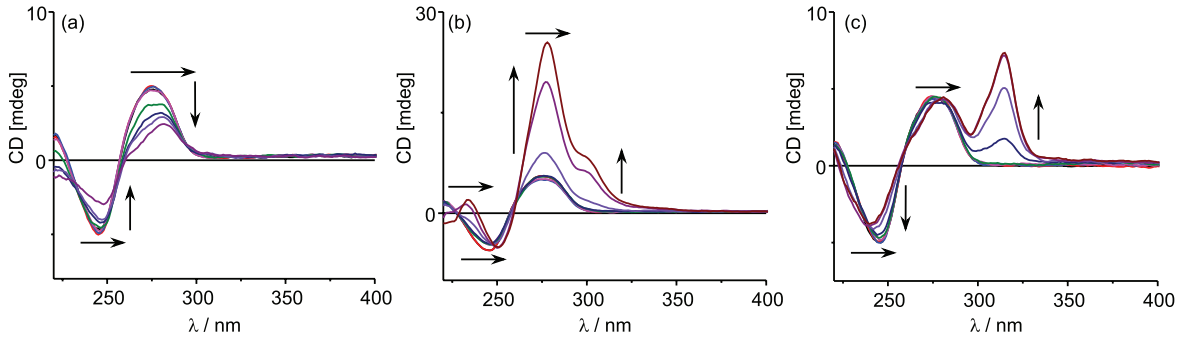

Figure 11. Circular dichroism of CT-DNA titrated with (a) **1**; (b) **2** and (c) **3** in concentrations ranging from 19.80 to 181.82 μmol L^{-1} (molar ratios of 0.10 to 1.00) and 0 (NC). The complexes **1**, **2** and **3** showed different results due to different interaction forms.

the characteristic bands of absorption of Phen and Bipy, respectively. Complex **1** presented no significant absorbance (data not shown). The hypochromism presented by **2** (Figure 12a) and **3** (Figure 12b) in the presence of increasing CT-DNA concentrations is characteristic of strong interactions.[54] The results obtained by the incubation of **3** (Figure 12b) in the presence of CT-DNA showed maximum absorption at λ 310 nm, with reduction of intensity by addiction of the complex, but an increment occurred in λ 260 nm. These events are characteristic

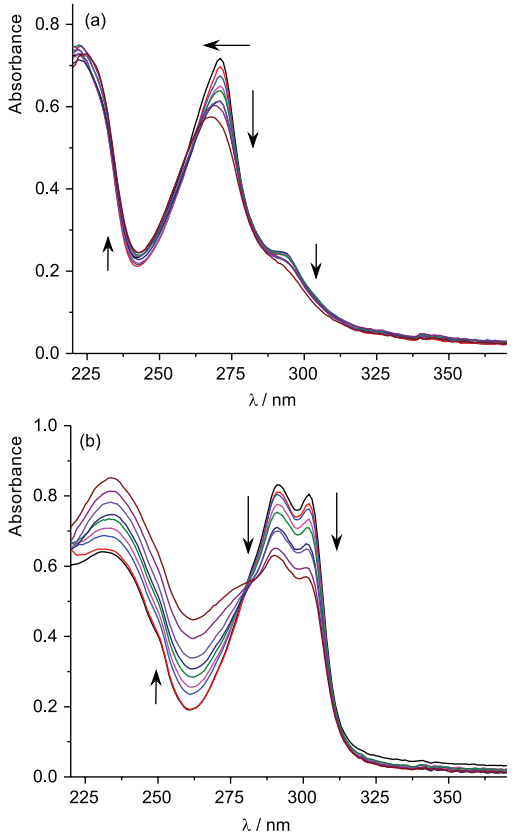

Figure 12. Spectrophotometric wave scan of (a) **2** and (b) **3** incubated in concentration of the complex of 50 μmol L^{-1} at growing concentrations of CT-DNA (0, 12.5, 25.0, 37.5, 50.0, 66.5, 75.0, 87.5 and 100 μmol L^{-1}). Both complexes presented a decrease on their absorption bands indicating their interaction with DNA.

to π-π* transitions for the pyridine rings.[62] These results are in agreement to the ones obtained from circular dichroism analysis, where a new band of absorption due to an unknown form of DNA in incubations of growing concentrations of **3** can be observed.

UV-Vis spectrophotometry is a useful method to determine the binding mode between metal complexes-DNA. In order, complex-DNA binding constants (K_b) were obtained according to equation 2.[63]

$$\frac{[DNA]}{(\varepsilon_a - \varepsilon_f)} = \frac{[DNA]}{(\varepsilon_b - \varepsilon_f)} + \frac{1}{K_b(\varepsilon_b - \varepsilon_f)} \quad (2)$$

According to İnci *et al.*,[63] [DNA] is the concentration of DNA in terms of base pairs (μmol L^{-1}), ε_a is the apparent extinction coefficient obtained by calculating A_{obs}/[complex], ε_f corresponds to the extinction coefficient of the complex in its free form, and ε_b refers to the extinction coefficient of the complex in the bound form. Each set of data, when fitted to the above equation, gave a straight line with a slope of $1/(\varepsilon_b - \varepsilon_f)$ and a *y*-intercept of $1/K_b(\varepsilon_b - \varepsilon_f)$. The K_b values are shown on Table 1. These results are in agreement with the results obtained with other complexes, where complexes containing 1,10-phenantroline present a K_b stronger than its counterpart containing 2,2'-bipyridine.[2,55] They are also in agreement with the cytotoxicity results where it is shown that **2** presents stronger cytotoxicity than **3**.

Table 1. Binding constants (K_b) for the interactions of complexes and CT-DNA

Compound	K_b	λ_{max} / nm
2	1.75×10^5	272
3	3.20×10^4	291

Cytotoxicity tests

The fact that copper complexes are able to directly interact and cleave DNA molecule encouraged us to study

their cytotoxicity in mammalian cell. Thus, MTT and clonogenic assays were performed to evaluate the influence of copper complexes and the prototype compound NaValp on the V79 cell viability.

MTT assay is an indirect cell survival analysis based on the mitochondrial activity and clonogenic method determines the cell viability based on the ability of a single cell to grow into a colony.[48,49] In both assays, cells were exposed for 72 h to NaValp and its complexes **1**, **2** and **3**. The higher concentrations were based on their maximum solubility. MTT and clonogenic results showed that the Cu^{II} complexes were able to decrease the cell viability in a dose-response manner after 72 h of exposure (Figures 13 and 14). The complexes **1**, **2** and **3** showed cytotoxic effects in the majority of the concentrations used in MTT and clonogenic assays. Among these compounds, similar toxicity was observed for **1** and **3**, where the half maximal inhibitory concentration (IC_{50}) values were 193 and 150 μmol L^{-1} to MTT (Figure 13) or 150 and 153 μmol L^{-1} to clonogenic assay (Figure 14), respectively. By direct comparison, **2** presented cytotoxicity at least 20 times higher than the others copper complexes, with IC_{50} values of 6.70 and 3.98 μmol L^{-1} to MTT and to clonogenic assay, respectively. Similar results were obtained with sulfonamide containing complexes. The ones synthesized with1,10-phenantroline presented minimal inhibitory concentrations (MIC) of 4.9 and 6.3 μmol L^{-1} and the one with 2,2-bipyridine inhibited the cell growth at the concentration of 129.3 μmol L^{-1} in HT29 cells.[64] Another example with similar results were obtained using copper *o*-phtalate complexes containing both diimines, where the MIC values were 5.5 and 75.3 μmol L^{-1}, respectively.[5] Interestingly, NaValp induced a decrease of about 20-60% in cell viability when cells were exposed to concentrations greater than 1000 μmol L^{-1}. The cytotoxicity of the diimines presented similar results as the complexes with values of 2.5 and 50.0 μmol L^{-1} in the MTT test and 2.5 and 100 μmol L^{-1} for 1,10-phenantroline and 2,2-bipyridine, respectively. The results that agree to the ones observed with HT29 cells indicates that the toxicity of the complexes is probably due to these ligands.

In contrast, when colony formation was analyzed, NaValp induced a weak cytotoxic effect between 10-20% when used at 1500 μmol L^{-1} or greater concentrations. This fact may be due to the decrease in the colony size observed in the cultures exposed to NaValp mainly at 1000 μmol L^{-1} or greater concentrations (data not shown), suggesting that cells did not grow at the same rate than the negative control group. Small colonies were also observed in the

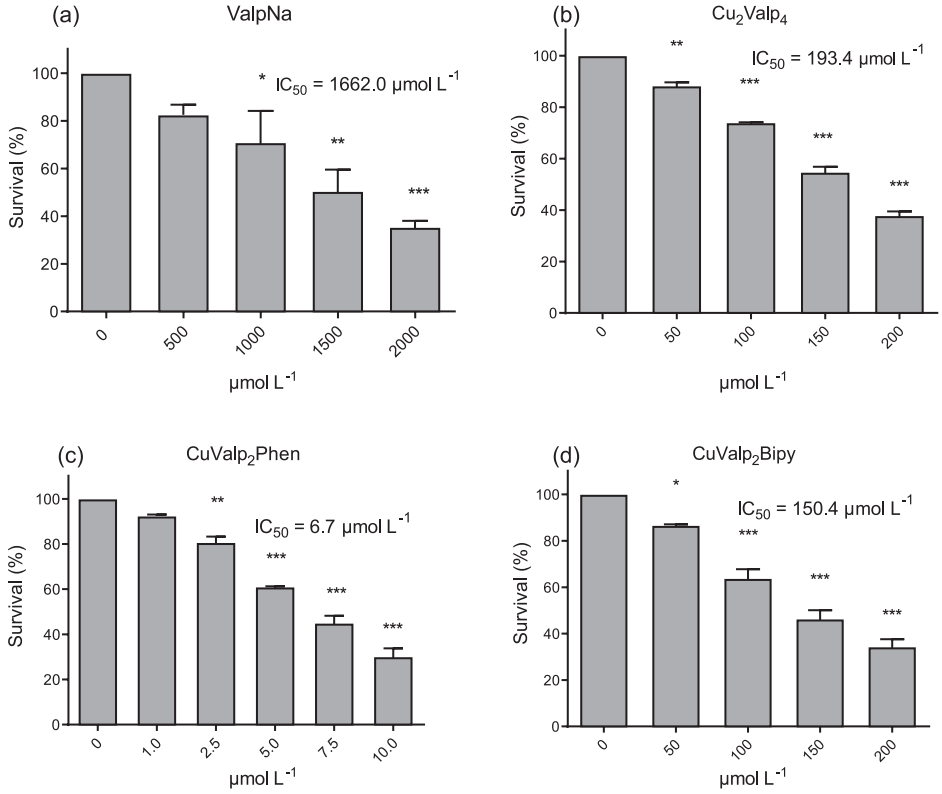

Figure 13. Dose-dependent cytotoxicity of NaValp and its complexes **1**, **2** and **3** in V79 cells as determined by MTT reduction method (percentage of negative control). Cells were exposed to NaValp (a), **1** (b), **2** (c) and **3** (d) at described concentrations for 72 h. Respective negative controls (solvents) were included; data are expressed as mean ± S.D., n = 3. *Data statistically significant different in relation to the negative control group *$p < 0.05$, **$p < 0.01$, ***$p < 0.001$/one-way ANOVA Dunnett's multiple comparison test.

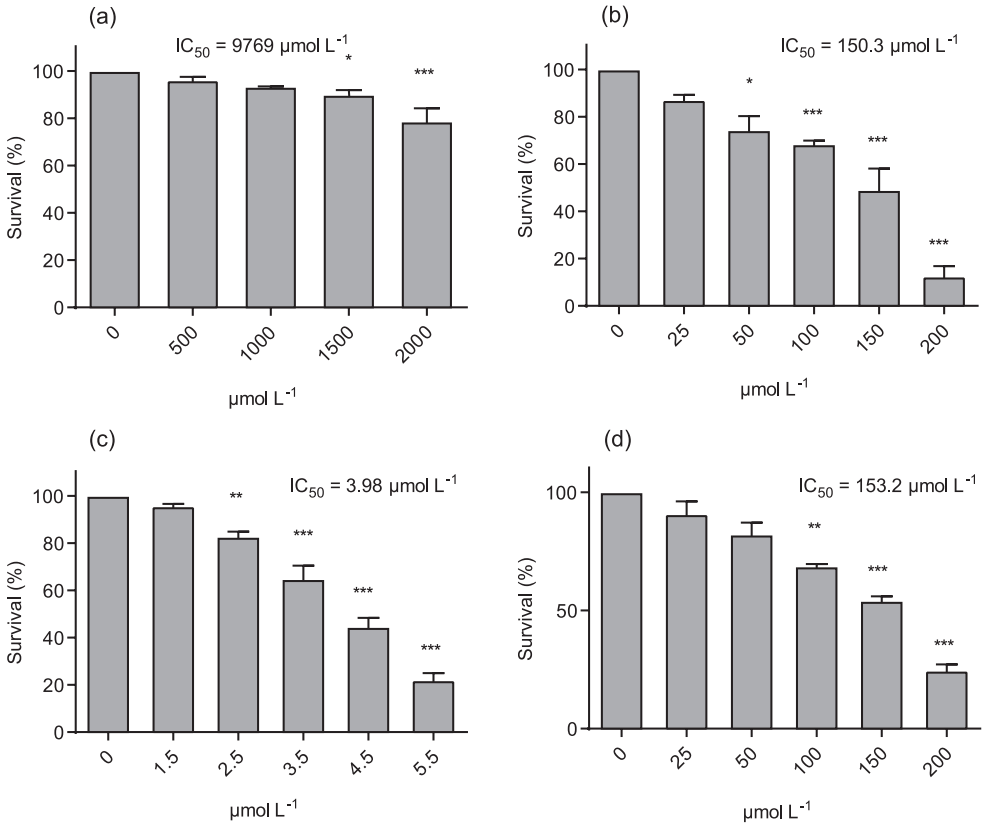

Figure 14. Clonogenic survival of V79 cells exposed to NaValp and its complexes **1**, **2** and **3**. Cells were exposed to NaValp (a), **1** (b), **2** (c) and **3** (d) for 72 h. Respective negative controls (solvents) were included; data are expressed as mean ± S.D., n = 3. *Data statistically significant different in relation to the negative control group *$p < 0.05$, **$p < 0.01$, ***$p < 0.001$/one-way ANOVA Dunnett's multiple comparison test.

cultures exposed to 50 µmol L^{-1} **1** and **3** and to 2.5 µmol L^{-1} **2** (data not shown), which may be also related to cell cycle alteration induced by NaValp, as described.[9,48,65-67] Therefore, it is shown that copper complexes were more cytotoxic than the NaValp, the prototype molecule, in V79 cells.

DNA interaction and single and double breaks can promote cell cycle arrest due to the necessity of the cell to remove the complexes or repair the lesions before duplicating its DNA. Once that all 3 complexes promote DNA cleavage in AL conditions, Cu^{II} is known as an oxidative agent and VPA reduces DNA repair, it was expected that cells incubated in presence of these substances would show slowing or absence of growing this result.[8,10,22,68,69] The stronger inhibition results obtained using **2** can be due to the intercalation properties of the complex that not necessary promote DNA cleavage in the assays with plasmidial DNA.

Conclusions

The VPA used in seizure, bipolar disorder and migraine headaches therapy has been reported in the last years as a drug candidate to be used in cancer therapy, alone or as an adjuvant. This new VPA therapeutic activity is probably linked to its epigenetic modulation effect by inhibiting histone deacetylation, and consequently, disturbing several molecular pathways. Supporting these findings, VPA has been demonstrating inhibitory activity on DNA repair and proliferation and also induction of ROS, DNA double strand breaks and cell death (mainly by apoptosis).[9,10,22,65]

Among metals which have been investigated on anticancer research, Cu^{II} has demonstrated promising effects in a variety of experimental models. Cu^{II} complexes were able to improve the cisplatin antitumor efficacy and this effect has been related to Cu^{II} redox activity.[5] Based on VPA and Cu^{II} pharmacological properties, a new group of Cu^{II} complexes has been synthesized with mixed ligands that were first thought to enhance the neurological effects of the original drug. However, as VPA has also demonstrated anticancer effects, this work aimed to evaluate the cytotoxic and DNA damaging profile of VPA and three binary and ternary Cu^{II} complexes of VPA with Phen or Bipy. By using different approaches, different profiles among VPA and all three Cu^{II}-VPA complexes were observed regarding DNA interaction, redox potential and cytotoxicity.

Whereas NaValp was not able to induce DNA breaks or conformational changes, Cu^{II} complexes were able to

cleave cell-free DNA in a nonspecific pattern, which was more pronounced in the presence of UV, suggesting they can be photo activated (Figures 5, 7 and 10). These findings may suggest that **1**, **2** and **3** lead to DNA cleavage through an oxidative insult. Nonetheless, this effect is unlikely to be related to the ROS, since the DNA breaks content was not altered when Cu^{II} complexes were incubated with DNA in oxygen absent conditions (Figure 9). Furthermore, Cu^{II} complexes were able to interfere on DNA structure, suggesting a groove binding activity for complex **1**, an intercalating profile for **2** and electrostatic interactions for **3** (Figure 11). In contrast, NaValp did not affect the DNA circular dichroism absorbance profile (Figure S9, SI section). These results corroborate with previous reports where oxidative and DNA binding has been shown by different Cu^{II} complexes.[5,7,19,55]

Regarding the cell viability results obtained in mammalian cell line V79, it was evidenced a clear and substantial difference among NaValp and Cu^{II} complexes. Complexes **1**, **2** and **3** were able to induce viability decrease when cells were exposed to concentrations of 50, 2.5 and 100 μmol L^{-1}, respectively. In contrast, NaValp decreased the cell viability only when used at concentrations equal or over 1000 μmol L^{-1} (Figures 13 and 14). By comparing the IC_{50} values of the compounds, we may suggest that the copper inclusion on the NaValp was responsible for the increasing of about 8 times on the cytotoxic activity of the prototype molecule. Moreover, Cu^{II} associated to Phen was able to increase at least 248 times the cytotoxicity of NaValp.

Taken together, the biological results are in accordance with the physical-chemical data, where the three Cu^{II} complexes demonstrated different DNA interaction and cytotoxicity patterns in relation to NaValp. In addition, the results might suggest that the underlying mechanism of the cytotoxic effects observed among the complexes could be related to their DNA interaction and damaging effects. As mentioned before, all Cu^{II} complexes presented DNA cleavage properties. Notably, **1** demonstrated activity on DNA conformation acting as groove binder and **3** as electrostatic binder. On the other hand, **2** was able to alter the DNA structure as a typical intercalator agent. Considering the possible different influences of binding or intercalation effects on the DNA conformation, the three Cu^{II} complexes may be able to induce different effects on critical process like transcription and replication. Therefore, the probable intercalation of **2** into DNA might be associated to its high cytotoxic profile, whereas the DNA binding interaction of **1** and **3** is less harmful to the cell survival. In this way, the DNA interaction potential may represent the key response to the cytotoxic results observed for the complexes, where the cytotoxic profile was: **2** greater than **3** greater than **1**.

In summary, this work reports a binary and two ternary Cu^{II} complexes of VPA with Phen or Bipy, which interacts with DNA promoting its cleavage and have an enhanced cytotoxicity when comparing to the putative anticancer drug VPA. Thus, these findings indicate their potential role as chemotherapeutic agents and demonstrated the capacity of these complexes to be photo activated, which offers the possibility of its use as photodynamic therapy agents.

Supplementary Information

Supplementary data of crystallographic study (Table S1), 2D and 3D statistical graphs of broken DNA (Figures S1-S8), circular dichroism graphs of CT-DNA (Figures S9-S13) and UV-Vis absorbance profile of CT-DNA (Figure S14) are available free of charge at http://jbcs.sbq.org.br as PDF file.

Crystallographic data (excluding structure factors) for the structures in this work were deposited in the Cambridge Crystallographic Data Centre as supplementary publication number CCDC 1507321. Copies of the data can be obtained, free of charge, via www.ccdc.cam.ac.uk/conts/retrieving.html or from the Cambridge Crystallographic Data Centre, CCDC, 12 Union Road, Cambridge CB2 1EZ, UK; fax: +44 1223 336033. E-mail: deposit@ccdc.cam.ac.uk.

Acknowledgments

The authors gratefully acknowledge financial support from CNPq, FAPERGS-PRONUPEQ process 16/2551-0000523-0, CAPES, SCIT (Brazil), and from CNRS, MENRT and LabEx LERMIT (ANR-10-LABX-33) (France). The authors also acknowledge the support from Ciência sem Fronteiras program to F. D., S. M., J. A. P. H. and P. R. S. (Brazil).

References

1. Grif, D. M.; Duff, B.; Suponitsky, K. Y.; Kavanagh, K.; Morgan, M. P.; Egan, D.; Marmion, C. J.; *J. Inorg. Biochem.* **2011**, *105*, 793.
2. Silva, P. P.; Guerra, W.; Silveira, J. N.; Ferreira, A. M. D. C.; Bortolotto, T.; Fischer, F. L.; Terenzi, H.; Neves, A.; Pereira-Maia, E. C.; *Inorg. Chem.* **2011**, *50*, 6414.
3. Monneret, C.; *Ann. Pharm. Fr.* **2011**, *69*, 286.
4. Jiang, Q.; Xiao, N.; Shi, P.; Zhu, Y.; Guo, Z.; *Coord. Chem. Rev.* **2007**, *251*, 1951.

5. Kellett, A.; Howe, O.; O'Connor, M.; McCann, M.; Creaven, B. S.; McClean, S.; Foltyn-Arfa Kia, A.; Casey, A.; Devereux, M.; *Free Radical Biol. Med.* **2012**, *53*, 564.
6. Marzano, C.; Pellei, M.; Tisato, F.; Santini, C.; *Adv. Anticancer Agents Med. Chem.* **2009**, *9*, 185.
7. Denoyer, D.; Masaldan, S.; la Fontaine, S.; Cater, M. A.; *Metallomics* **2015**, *7*, 1459.
8. Santini, C.; Pellei, M.; Gandin, V.; Porchia, M.; Tisato, F.; Marzano, C.; *Chem. Rev.* **2014**, *114*, 815.
9. Diederich, M.; Chateauvieux, S.; Morceau, F.; Dicato, M.; *J. Biomed. Biotechnol.* **2010**, *2010*, 201.
10. Wang, Y.; Kuramitsu, Y.; Kitagawa, T.; Tokuda, K.; Baron, B.; Akada, J.; Nakamura, K.; *Target. Oncol.* **2015**, *10*, 575.
11. Rogolino, D.; Cavazzoni, A.; Gatti, A.; Tegoni, M.; Pelosi, G.; Verdolino, V.; Fumarola, C.; Cretella, D.; Petronini, P. G.; Carcelli, M.; *Eur. J. Med. Chem.* **2017**, *128*, 140.
12. Mukherjee, N.; Podder, S.; Banerjee, S.; Majumdar, S.; Nandi, D.; Chakravarty, A. R.; *Eur. J. Med. Chem.* **2016**, *122*, 497.
13. Buchtík, R.; Trávníček, Z.; Vančo, J.; Herchel, R.; Dvořák, Z.; *Dalton Trans.* **2011**, *40*, 9404.
14. Cadoni, E.; Valletta, E.; Caddeo, G.; Isaia, F.; Grazia, M.; Vascellari, S.; Pivetta, T.; *J. Inorg. Biochem.* **2017**, *173*, 126.
15. Kowol, C. R.; Keppler, B. K.; Hartinger, C. G.; Jungwirth, U.; *Antioxid. Redox Signaling* **2011**, *15*, 1085.
16. Bencini, A.; Lippolis, V.; *Coord. Chem. Rev.* **2010**, *254*, 2096.
17. Zhou, X. Q.; Li, Y.; Zhang, D. Y.; Nie, Y.; Li, Z. J.; Gu, W.; Liu, X.; Tian, J. L.; Yan, S. P.; *Eur. J. Med. Chem.* **2016**, *114*, 244.
18. Rajalakshmi, S.; Kiran, M. S.; Nair, B. U.; *Eur. J. Med. Chem.* **2014**, *80*, 393.
19. Bortolotto, T.; Silva-Caldeira, P. P.; Pich, C. T.; Pereira-Maia, E. C.; Terenzi, H.; *Chem. Commun.* **2016**, *52*, 7130.
20. Bortolotto, T.; Silva, P. P.; Neves, A.; Pereira-Maia, E. C.; Terenzi, H.; *Inorg. Chem.* **2011**, *50*, 10519.
21. Hardman, J. G.; Limbird, L. E.; Gilman, A. G.; *Goodman & Gilman: As Bases Farmacológicas da Terapêutica*, 11ª ed.; McGraw-Hill: Rio de Janeiro, 2012.
22. Groselj, B.; Sharma, N. L.; Hamdy, F. C.; Kerr, M.; Kiltie, A. E.; *Br. J. Cancer* **2013**, *108*, 748.
23. Wolf, K.; Ide, N.; Koufopoulos, J.; Williams, R. J.; Tse, T.; *NLM Tech. Bull.* **2017**, *416*, e4; https://clinicaltrials.gov/ct2/results?term=valproic+acid&Sear ch=Search accessed on May 20, 2017.
24. Hadjikostas, C. C.; Katsoulos, C. A.; Sigalas, M. P.; Tsipis, C. A.; *Inorg. Chim. Acta* **1990**, *167*, 165.
25. Abuhijleh, A. L.; Woods, C.; *Inorg. Chim. Acta* **1993**, *209*, 187.
26. Doedens, R. J.; *Progress in Inorganic Chemistry*, vol. 21, 1st ed.; Interscience: New York, 1976.
27. Sylla-Iyarreta Veitía, M.; Dumas, F.; Morgant, G.; Sorenson, J. R. J.; Frapart, Y.; Tomas, A.; *Biochimie* **2009**, *91*, 1286.
28. Veitía, S. I. M.; Dumas, F.; Morgant, G.; *US pat. 2012/0142658A1* **2012**.
29. Abuhijleb, A. L.; *J. Inorg. Biochem.* **1997**, *68*, 167.
30. Grünspan, L. D.; Mussulini, B. H. M.; Baggio, S.; dos Santos, P. R.; Dumas, F.; Rico, E. P.; de Oliveira, D. L.; Moura, S.; *Epilepsy Res.* **2018**, *139*, 171.
31. Tan, M. W.; Rahme, L. G.; Sternberg, J. A.; Tompkins, R. G.; Ausubel, F. M.; *Proc. Natl. Acad. Sci. U. S. A.* **1999**, *96*, 2408.
32. QIAGEN; *QIAGEN® Plasmid Purification Handbook*; QIAGEN, 2012. Available at https://www.qiagen.com/kr/resources/resourcedetail?id=46205595-0440-459e-9d93-50eb02e5707e&lang=en, accessed in November 2018.
33. *ADABS Software*; Bruker-AXS, Madison, WI, USA, 2007.
34. *SADABS Software*; Bruker-AXS, Madison, WI, USA, 2007.
35. Blessing, R.; *SORTAV*; Medical Foundation Buffalo, New York, USA, 1995
36. Altomare, A.; Cascarano, G.; Giacovazzo, C.; Guagliardi, A.; *J. Appl. Crystallogr.* **1993**, *26*, 343.
37. Altomare, A.; *SIR94*; Instituto di Ricerca per lo Sviluppo di Metodologie Cristalografiche CNR, University of Bari, Italy, 1999.
38. Sheldrick, G. M.; *SHELX97, Program for the Refinement of Crystal*; University of Goettingen, Germany, 2008.
39. Farrugia, L. J.; *WinGX Package, Programs for the Treatment of Small-Molecule Single-Crystal Diffraction Data*; University of Glasgow, Glasgow, Scotland, 2012.
40. *OriginPro 2016*, version b9.3.226 (test version); OringinLab Corporation, USA, 2016.
41. Al-Mogren, M. M.; Alaghaz, A.-N. M. A.; Ebrahem, E. A.; *Spectrochim. Acta, Part A* **2013**, *114*, 695.
42. Dean, J. A.; *Lange's Handbook of Chemistry*, 15th ed.; McGraw-Hill: New York, 1999.
43. Ausubel, F. M.; Brent, R.; Kingston, R. E.; Moore, D. D.; Seidman, J. G.; Smith, J. A.; Struhl, K.; *Short Protocols in Molecular Biology: A Compendium of Methods from Current Protocols in Molecular Biology*, 2nd ed.; John Wiley & Sons: New York, 2002.
44. Neves, A.; Terenzi, H.; Horner, R.; Horn, A.; Szpoganicz, B.; Sugai, J.; *Inorg. Chem. Commun.* **2001**, *4*, 388.
45. *Design-Expert®*, version 7.0; Stat-Ease Inc., USA, 2016.
46. Rey, N. A.; Neves, A.; Silva, P. P.; Paula, F. C. S.; Silveira, J. N.; Botelho, F. V.; Vieira, L. Q.; Pich, C. T.; Terenzi, H.; Pereira-Maia, E. C.; *J. Inorg. Biochem.* **2009**, *103*, 1323.
47. Li, J. H.; Wang, J. T.; Hu, P.; Zhang, L. Y.; Chen, Z. N.; Mao, Z. W.; Ji, L. N.; *Polyhedron* **2008**, *27*, 1898.
48. Denizot, F.; Lang, R.; *J. Immunol. Methods* **1986**, *89*, 271.
49. Franken, N. P.; Rodermond, H. M.; Stap, J.; Haveman, J.; van Bree, C.; *Nat. Protoc.* **2006**, *1*, 2315.
50. *Prism®*, version 6.01; GraphPad Inc., USA, 2016.
51. Darawsheh, M.; Abu Ali, H.; Abuhijleh, A. L.; Rappocciolo, E.; Akkawi, M.; Jaber, S.; Maloul, S.; Hussein, Y.; *Eur. J. Med. Chem.* **2014**, *82*, 152.

52. Haynes, W. M.; Lide, D. R.; Bruno, T. J.; *CRC Handbook of Chemistry and Physics*, 97th ed.; CRC PRESS: Boca Raton, 2016.
53. Albani, B.; Peña, B.; Leed, N.; de Paula, N. B. G.; Pavani, C.; Baptista, M. S.; Dunbar, K. R.; Turro, C.; *J. Am. Chem. Soc.* **2014**, *136*, 17095.
54. Ramakrishnan, S.; Rajendiran, V.; Palaniandavar, M.; Periasamy, V. S.; Srinag, B. S.; Krishnamurthy, H.; Akbarsha, M. A.; *Inorg. Chem.* **2009**, *48*, 1309.
55. Silva, P. P.; Guerra, W.; dos Santos, G. C.; Fernandes, N. G.; Silveira, J. N.; Ferreira, A. M. C.; Bortolotto, T.; Terenzi, H.; Bortoluzzi, A. J.; Neves, A.; Pereira-Maia, E. C.; *J. Inorg. Biochem.* **2014**, *132*, 67.
56. Rey, N. A.; Neves, A.; Bortoluzzi, A. J.; Pich, C. T.; Terenzi, H.; *Inorg. Chem.* **2007**, *46*, 348.
57. Kovacic, R. T.; Welch, J. T.; Franklin, S. J.; *J. Am. Chem. Soc.* **2003**, *125*, 6656.
58. Berova, N.; Nakanishi, K.; Woody, R. W.; *Circular Dichroism: Principles and Applications*, 2nd ed.; WileyVCH: New York, 2000.
59. Dhar, S.; Nethaji, M.; Chakravarty, A. R.; *J. Inorg. Biochem.* **2005**, *99*, 805.
60. Ganeshpandian, M.; Loganathan, R.; Ramakrishnan, S.; Riyasdeen, A.; Akbarsha, M. A.; Palaniandavar, M.; *Polyhedron* **2013**, *52*, 924.
61. Gawroński, J.; Grajewski, J.; *Org. Lett.* **2003**, *5*, 3301.
62. Vila Nova, S. P.; Pereira, G. A. L.; Sá, G. F.; Alves Jr., S.; Bazin, H.; Autiero, H.; Mathis, G.; *Quim. Nova* **2004**, *27*, 709.
63. İnci, D.; Aydın, R.; Vatan, Ö.; Sevgi, T.; Yılmaz, D.; Zorlu, Y.; Yerli, Y.; Çoşut, B.; Demirkan, E.; Çinkılıç, N.; *J. Biol. Inorg. Chem.* **2017**, *22*, 61.
64. Nakahata, D. H.; de Paiva, R. E. F.; Lustri, W. R.; Ribeiro, C. M.; Pavan, F. R.; da Silva, G. G.; Ruiz, A. L. T. G.; de Carvalho, J. E.; Corbi, P. P.; *J. Inorg. Biochem.* **2018**, *187*, 85.
65. Tung, E. W. Y.; Winn, L. M.; *Reprod. Toxicol.* **2011**, *32*, 255.
66. Hrebackova, J.; Hrabeta, J.; Eckschlager, T.; *Curr. Drug Targets* **2010**, *11*, 361.
67. Mawatari, T.; Ninomiya, I.; Inokuchi, M.; Harada, S.; Hayashi, H.; Oyama, K.; Makino, I.; Nakagawara, H.; Miyashita, T.; Tajima, H.; Takamura, H.; Fushida, S.; Ohta, T.; *Int. J. Oncol.* **2015**, *47*, 2073.
68. Tian, Y.; Liu, G.; Wang, H.; Tian, Z.; Cai, Z.; Zhang, F.; Luo, Y.; Wang, S.; Guo, G.; Wang, X.; Powell, S.; Feng, Z.; *DNA Repair* **2017**, *58*, 1.
69. Hureau, C.; Faller, P.; *Biochimie* **2009**, *91*, 1212.

Submitted: July 21, 2018
Published online: November 22, 2018